JAST
Journal of Aerospace Science and Technology

Pages:110-118 / Vol. 15/ No. 2 /Summer- Fall 2022

Journal of Aerospace Science and Technology

www:jast.ias.ir

Scienctifie-Research Article

Buckling Behavior of Functionally Graded Nano Clay-Reinforced Composite Beams

Mahdi Karami Khorramabadi[1]* , **Ali Reza Nezamabadi**[2]

1-Department of Mechanical Engineering, Khorramabad Branch, Islamic Azad University, Khorramabad, Iran
2- Department of Mechanical Engineering, Arak Branch, Islamic Azad University, Arak, Iran

ABSTRACT

This paper investigates the buckling behavior of functionally graded nanocomposite beams reinforced by nano clay. Accordingly, the specimens were prepared, and the experimental tensile and buckling tests were carried out. The Young's modulus of epoxy/clay nanocomposite for functionally graded and uniformly distribution nano clay are estimated through a model based on the genetic algorithm approach. Also, the first-order shear deformation beam theory is applied for a simply supported beam, and the governing equations are derived using the Hamilton principle. Moreover, the influence of nanoparticles on the buckling load of a beam is presented. A comparison study is conducted to assess the efficacy and accuracy of the present analysis. A comparison of theoretical analysis with the experimental results demonstrated high accuracy.

Keywords:*Buckling, Functionally graded nanocomposite, Epoxy, Genetic algorithm theory.*

Introduction

Nanocomposite structures exhibit superior properties such as high strength/stiffness to weight ratio and greater resistance to environmental degradation compared to conventional metallic materials. Hence, they are widely used in aerospace, naval, civil, and mechanical engineering applications. The use of high-strength materials in such applications leads to slender sections, thus making buckling a primary mode of failure of the member when subjected to axial compressive forces. In addition to the filler properties, the material properties of polymer nanocomposites are largely dependent on the interface area and intensity of intermolecular interaction between the filler and matrix. However, in recent years polymer matrix-based nanocomposites have been attracting researchers' attention by offering properties significantly better than those of conventional particulate or fibrous polymeric composites [1-2]. This greater interest is due to the fact that some types of nanoparticles are being incorporated into polymeric resins to fabricate materials with increased performance. The nanoscale particles possess enormous surface area. Hence, the interfacial area between the two intermixed phases in a nanocomposite is substantially larger than in traditional composites, which results in increased bonding between the particles and the matrix. As such, several nanocomposites' mechanical, thermal, and electrical properties are observed to be better than those of conventional micro composites or neat matrix resin [3–10]. The functionally graded material (FGM) is a novel type of composite

1 Assistant Professor (Corresponding author), mk.khorramabadi@iau.ac.ir
2 Assistant Professor

DOI : 10.22034/jast.2022.341613.1118
Submit: 09.05.2022 / Accepted: 08.10.2022
Print ISSN:1735-2134 Online ISSN: 2345-3648

material whose mechanical properties smoothly and continuously vary in a preferred direction [11-14].

With a reasonable graded distribution, the dispersion of nanofillers in the polymer matrix can effectively use reinforcements. To address the effects of nanofiller distributions on the mechanical behaviors of functionally graded (FG) polymer-based nanocomposites, different types of distributions have been introduced and employed in the literature, such as the uniform distribution (UD), FG-V shape, FG-O shape, and FG-X shape [15-20]. All existing functions to describe the nanofiller distribution law are not adjustable since no adjustable parameter is included. The distribution law with adjustable parameters can lead to continuously graded mechanical properties for the nanofiller-reinforced polymer nanocomposites. However, no such law has been reported yet. An adjustable distribution is believed to have great potential for introducing a novel type of nanocomposite and can be used to optimize the mechanical performances of the nanofiller-reinforced structures.

This work studies the mechanical buckling of functionally graded (FG) nanocomposite beams reinforced by nano clay. To this end, the specimens were prepared, and the experimental tensile and buckling tests were carried out. The Young's modulus of epoxy/clay nanocomposite for functionally graded and uniformly distribution nano clay are estimated through a model based on the genetic algorithm approach. Also, the first-order shear deformation beam theory is applied for a simply supported beam, and the governing equations are derived using the Hamilton principle. Moreover, the influence of nanoparticles on the buckling load of a beam is presented. A comparison study is conducted to assess the efficacy and accuracy of the present analysis. A comparison of theoretical analysis with the experimental results demonstrated high accuracy.

Experimental Procedure

The specimens were tested according to ASTM D638 with three repeats. The tension tests were carried out using a Gotech universal testing machine (Model GT-AI5000L) with a crosshead speed of 50 mm/min.

Materials

The polymer matrix used in this study was an Epoxy with the trade name PR7000 made by AL TANNA Co. (Germany), with a density of $\rho = 2.25 g/ml$. The hardener was mixed in a ratio of 10:1. The nanofiller was US7810 made by U.S. Research Nanomaterials Inc., USA.

Mechanical properties

The material compositions of the nanocomposites for uniform distribution are listed in Table 1. In this table, wt.% is considered as the weight percent.

Table 1: Sample compositions

Sample No.	Epoxy (wt%)	Nano Clay (wt%)
1	100	-
2	97	3
3	95	5
4	93	7

For FG distribution, the preparation procedure for uniform distribution was done for samples with 1 mm thicknesses. The thickness of each sheet was 1 mm and four sheets with different nano particles weight percent (pure, 3 wt%, 5 wt%, and 7 wt%) were used to make FG nanocomposite. The values of the nanocomposites' Young's modulus for FG and uniform distribution of nano clay are shown in Fig.1.

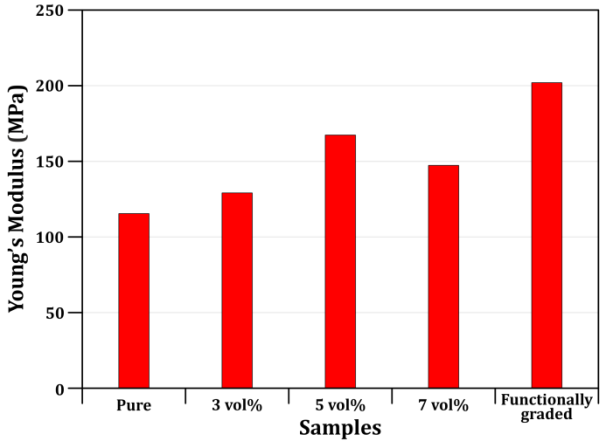

Figure 1: Young's modulus of nanocomposites with different distributions of nanoparticles

It is shown that Young's modulus begins to increase up to 5 wt% of nano clay and then decreases. Therefore, Young's modulus is generally larger for FG distribution than the corresponding values for uniform distribution of

nano clay. The agglomeration of nano clay particles on a 7 wt% percentage of nano clay can be seen in epoxy/clay nanocomposite. This effect verifies the decrement of Young's modulus compared with other specimens.

Mechanical Buckling Tests

The mechanical buckling tests were carried out on columns made from FG and uniformly distribution nanocomposite using a beam apparatus from TQ, England (Model SM1005). The test specimens had a rectangular cross-section $0.02\text{m} \times 0.004$ m and a length of 0.2m with simply supported at both ends.

Mathematical Modeling

In computer science and operations research, genetic algorithm (GA) is a metaheuristic inspired by the process of natural selection that belongs to the larger class of evolutionary algorithms (EA). Genetic algorithms are commonly used to generate high-quality solutions to optimization and search problems by relying on bio-inspired operators such as mutation, crossover, and selection. The GA method searches for the best alternative (in the sense of a given fitness function) through chromosome evolution [21]. The basic steps in the GA analysis are shown in Figure 2.

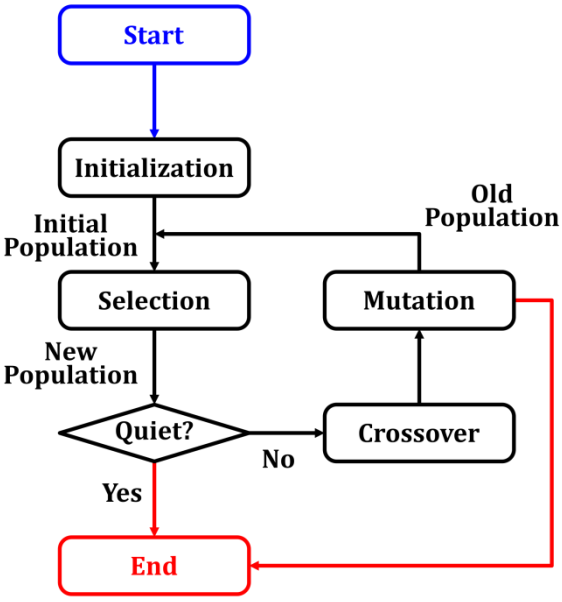

Figure 2: High-level description of the GA

As shown above, an initial population of chromosomes is randomly selected firstly. Then each chromosome in the population is evaluated in terms of its fitness (expressed by the fitness function). Next, a new population of chromosomes is selected from the given population by giving a greater chance to select chromosomes with higher fitness, called the reproduction operation. The new population may contain duplicates. If given stopping criteria are not met, including no chance in the old and new population and specified computing time, some specific genetic-like operations are performed on chromosomes of the new population. These operations produce new chromosomes called offspring. The same steps of this process, evaluation and reproduction operation, are then applied to the chromosomes of the resulting population. The whole process is repeated until the given stopping criteria are met. The best chromosome expresses the solution in the final population. In this paper, the "$1 - R^2_{adj}$" is introduced as a fitness function that is to be minimized. "R^2_{adj}" is the accuracy criterion of an arbitrary mechanical property function (such as Young's modulus). "R^2_{adj}" is defined as a process that is demonstrated below. The mechanical property is the function of a nano clay weight percentage and "R^2_{adj}" is a function of coefficients which are introduced below. M_i is considered as the mechanical properties and "W" as the nano clay weight percentage. The M_i is expressed as a polynomial function of "W" as follows:

$$M_i = \sum_{j=0}^{4} a_{ji} W^j \tag{3.1}$$

Now, the coefficients a_{ji} are found by maximizing the accuracy of a polynomial function. The equations can be written as:

$$R^2_{adj} = 1 - \frac{VAR_E}{VAR_T} \tag{3.2}$$

in which

$$VAR_E = SS_{Err}/(n - k - 1) \tag{3.3}$$

$$VAR_T = SS_{Tot}/(n - 1) \tag{3.4}$$

$$SS_{Tot} = \sum_{i=1}^{n} (y_i - \bar{y})^2 \tag{3.5}$$

$$SS_{Err} = \sum_{i=1}^{n} (y_i - M_i)^2 \quad (3.6)$$

$$\bar{y} = \frac{1}{n} \sum_{i=1}^{n} y_i \quad (3.7)$$

$$M_i(W) = a_{0i} + a_{1i}W + a_{2i}W^2 + a_{3i}W^3 \quad (3.8)$$

In the GA, the configuration chosen was as follows: $n = 4$ is the number of experiments and $k = 0$ is the number of duplicated experiments and y_i shows the experimentally measured mechanical properties. The crossover probability was equal to 0.8, and the probability of mutation was equal to 0.2 in equations. After minimization of "$1 - R^2_{adj}$" using MATLAB, factors a_{ji} are obtained after approximately 40 generations as the number of iterations. The initial values of a_{ji} which have been selected randomly are initial populations. Obtaining the a_{ji} coefficients, Young's modulus can be expressed as functions of nano clay weight percentage as follows:

$$E = -25.145w + 14.276w^2 + -1.432w^3 + 115.108 \quad (3.9)$$

Where, w is the nano clay weight percentage. To investigate the validation of the present results, comparison studies are carried out for the Young modulus of uniform distribution nanocomposites as presented in Table 2.

Table 2: Comparison of Young's modulus for uniform distribution nanocomposites

Nano clay weight percentage	Theoretical predictions (Mpa)	Experimental Results (Mpa)
pure	115.108	115.108
3%	129.493	129.486
5%	167.283	167.258
7%	147.441	147.379

The compression between theoretical predictions and experimental data shows the high accuracy of the present analysis. Equation 3.9 can be used to derive the suitable relation for Young's modulus of functionally graded distribution. The specimen with functionally graded distribution consists of four perfectly bonded sheets with a total thickness of 4 mm. Each sheet has 1 mm thickness with different nanoparticles weight fractions (pure, 3 wt.%, 5 wt.% and 7 wt.%). The Young's modulus can be written as:

$$E(z) = -25.145(2[z] + Sgn[z]) + 14.276(2[z] + Sgn[z])^2 + -1.432(2[z] + Sgn[z])^3 + 115.108 \quad (3.10)$$

As mentioned before, the Young modulus is assumed to vary as a function of the thickness coordinate z. After a simple variable change as $z = \bar{z} + 2$, the coordinate $\bar{z}$ changes within $-2 \le \bar{z} \le 2$. Equation 3.10 can be verified by employing the buckling analysis of functionally graded nanocomposite beams under axial compressive load.

Theoretical Formulation

The formulation is presented based on the assumptions of the first-order shear deformation beam theory. According to this theory, the displacement field can be written as [22]:

$$u(x,\bar{z}) = \bar{z}\phi(x)$$
$$w(x,\bar{z}) = w_0(x,\bar{z}) \quad (4.1)$$

Given the displacement field in Equation 4.1, the strain displacement relations are given by [22]:

$$\varepsilon_{xx} = \frac{\partial u}{\partial x} = \bar{z}\frac{d\phi}{dx}$$
$$\gamma_{xz} = \frac{\partial u}{\partial \bar{z}} + \frac{\partial w}{\partial x} = \phi + \frac{dw}{dx} \quad (4.2)$$

A functionally graded beam with rectangular cross-section is shown in Figure 3.

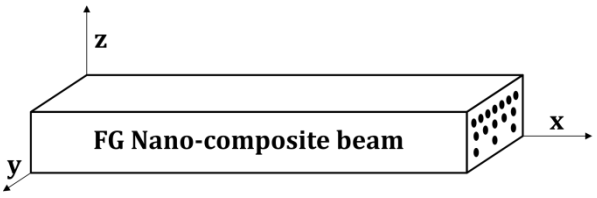

Figure 3: Schematic of the problem studied.

The thickness, length, and width of the beam are denote by $h, L,$ and b , respectively. The $x-y$ plane coincides with the midplane of the beam and the $\bar{z}$-axis located along the thickness direction.

The Young modulus E is assumed to vary as a function of the thickness coordinate variable $\bar{z}$ $(-2 \le \bar{z} \le 2)$. The constitutive relations for the functionally graded beam are given by [23]:

$$\sigma_{xx} = E(\bar{z})\varepsilon_{xx}$$
$$\sigma_{xz} = G(\bar{z})\gamma_{xz} \quad (4.3)$$

Where, σ_{xx}, σ_{xz}, $\mathrm{E}(\bar{z})$ and $\mathrm{G}(\bar{z})$ are the normal stress, shear stress, and the Young and shear modulus, respectively. The shear modulus can be written as [24]:

$$G(\bar{z}) = \frac{E(\bar{z})}{2(1+\nu)} \quad (4.4)$$

Where, ν is the Poisson ratio, estimated with the aid of the equation [25]:

$$\frac{\sigma_y}{E} = \frac{1-2\nu}{6(1+\nu)} \quad (4.5)$$

Where, σ_y is the yield strength and equals to 29.725 Mpa based on the tensile test result. In fact, The total yield strength for all functionally graded samples can be obtained from the tensile test and calculated using machine software like Young's modulus for functionally graded samples. Also, the Poisson ratio is assumed to be constant through the thickness of a beam [26]. So, equation 4.5 can be used to estimate the Poisson ratio for all samples. Also, u and w are the displacement components in the $x-$ and $\bar{z}$-directions, respectively.

The potential energy can be expressed as [22]:

$$U = \frac{1}{2}\int_v (\sigma_{xx}\varepsilon_{xx} + \sigma_{xz}\gamma_{xz})\,\mathrm{d}v \quad (4.6)$$

After substituting Equation (4.2) and Equation (4.3) with Equation (4.6) and neglecting the higher-order terms, we obtain

$$U = \frac{1}{2}\int_v [(E(\bar{z})\left(\bar{z}\frac{d\phi}{dx}\right))(\bar{z}\frac{d\phi}{dx}) + (G(\bar{z})(\phi + \frac{dw}{dx}))(\phi + \frac{dw}{dx})]dv \quad (4.7)$$

The width of a beam is assumed to be constant, which is obtained by integrating along y over v. Then, Equation (4.7) becomes

$$U = \frac{1}{2}\int_0^L [D\left(\frac{d\phi}{dx}\right)^2 + \frac{A}{2(1+\nu)}(\phi^2 + (\frac{dw}{dx})^2 + 2\phi\frac{dw}{dx})]dx \quad (4.8)$$

Where,

$$A = bK_s\int_{-\frac{h}{2}}^{+\frac{h}{2}} G(\bar{z})\mathrm{d}z \quad D = b\int_{-\frac{h}{2}}^{+\frac{h}{2}} \bar{z}^2 E(\bar{z})\mathrm{d}z \quad (4.9)$$

Where, A, D and K_s are the shear rigidity, flexural rigidity and shear correction factor, respectively. The beam is subjected to the axial compressive load P as shown in Figure 4. The work done by the axial compressive load can be expressed as [22]:

$$W = \frac{1}{2}\int_0^L P\left(\frac{\partial w}{\partial x}\right)^2 \mathrm{d}x \quad (4.10)$$

We apply the Hamilton principle to derive the equilibrium equations of beam as follows [23]:

$$\delta\int_0^t (T - U + W)\,\mathrm{d}t = 0 \quad (4.11)$$

Where, T is the kinetic energy. Substituting Equation (4.8) and Equation (4.10) into Equation (4.11) leads to the following equilibrium equations of the functionally graded beam based on the first-order shear deformation theory

$$(P - A)\frac{d^2w}{dx^2} - A(\frac{d\phi}{dx}) = 0 \quad (4.12)$$

$$D(\frac{d^2\phi}{dx^2}) - A(\phi + \frac{dw}{dx}) = 0 \quad (4.13)$$

Stability Analysis

The boundary conditions for the simply supported column are given by:

$$w = \frac{d^2w}{dx^2} = \frac{d\phi}{dx}, \qquad at \quad x = 0 \quad and \quad x = L \quad (5.1)$$

By differentiating Equation (4.13) and then using Equation (4.12), we obtain

$$D(\frac{d^3\phi}{dx^3}) = P(\frac{d^2w}{dx^2}) \quad (5.2)$$

Equation (4.12) can be solved for $\frac{d\phi}{dx}$

$$(\frac{d\phi}{dx}) = \frac{(P-A)}{A}(\frac{d^2w}{dx^2}) \quad (5.3)$$

By substituting Equation 5.3 into 5.2 and applying the boundary conditions, the smallest value of the critical buckling load of the nanocomposite beam is derived as follows, which gives a simple buckling mode and shape:

$$p_{cr} = \frac{(\frac{\pi}{L})^2 D}{1+(\frac{\pi}{L})^2 \frac{D}{K_s A}} \quad (5.4)$$

Where, K_s can be expressed as [26]:

$$K_s = \frac{5}{(6-(\nu_1 V_1 + \nu_2 V_2))} \quad (5.5)$$

Where, ν_1 and ν_2 are Poisson's ratios of the nano clay and the epoxy, respectively. Whereas, V_1 and V_2 are the nano clay and the epoxy volume fractions, respectively. The quantity of $(\nu_1 V_1 + \nu_2 V_2)$ for present nanocomposite is infinitesimal and the shear correction factor can be assumed to be $K_s = 5/6$ [27].

Results and Discussion

This paper investigates the mechanical buckling of the simply supported functionally graded nanocomposite beams based on the first-order shear deformation theory. The material compositions of the nanocomposite beam and Young's modulus are listed in Tables 1 and 2, respectively. Also, the effect of nanoparticles with different weight fractions on the Theoretical buckling load is shown in Figure 5. It is noticed that buckling loads for the beams with uniform distribution of nanocomposite are generally lower than the corresponding values for the beams with the functionally graded distribution of nanocomposites. Also, it is seen that increasing nanoparticles' weight percentage up to 5 wt% leads to an increase in the buckling loads for the beams with uniform distribution of nanoparticles. However, an increase in the amount of nano clay up to more than 5 wt% leads to a decrease in the buckling load.

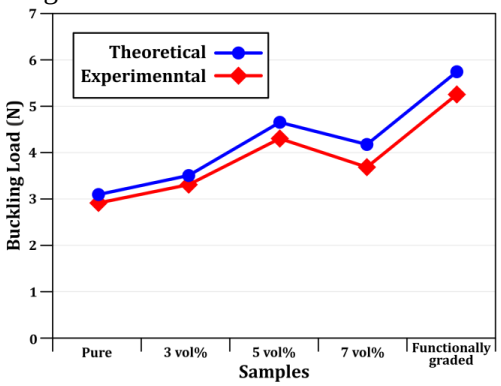

Figure 4: The effect of nanoparticles with different weight fractions on the buckling load

The comparison between theoretical and experimental data of buckling load for uniform and functionally graded distribution nanocomposites is shown in Table 3. As observed, there is good agreement between the results. Thus, the presented approach for analysis of mechanical buckling of uniform and functionally graded distribution nanocomposites has high accuracy.

Table 3: Compression between theoretical and the experimental data of buckling load

Nano clay (wt%)	Theoretical Buckling Load (N)	Experimental Buckling Load (N)	Percentage of Error (%)
pure	2.95	***3.1***	***4.8***
3%	3.38	***3.5***	***3.4***
5%	4.38	***4.7***	***6.8***
7%	3.78	***4.2***	***10***
FG	5.27	***5.8***	***9.1***

The results presented in Table 3 show that the percentage of errors between the theoretical and experimental results is acceptable. This difference is due to various factors, including the error related to Young's modulus modeling and the assumptions related to the displacement field.

Conclusions

This study investigates the mechanical buckling of epoxy/clay nanocomposite columns with uniform and functionally graded (FG) distributions of nano clay. Young's modulus for the FG distribution of nano clay was generally more significant than the corresponding value for the uniform distribution of nano clay. After increasing the nanoparticles' weight fractions, Young's modulus increased up to

5 wt.% nano clay. Also, increasing the amount of nano clay up to more than 5 wt% leads to a decrease in Young's modulus. Results show that GA can be considered an acceptable optimization research technique to identify Young's modulus of nanocomposites with maximum accuracy. The buckling load for the uniform distribution nanocomposite beam was generally lower than the corresponding value of FG distribution. The buckling load for uniform nanoparticles distribution of beam increased by increasing nanoparticles weight percent up to 5 wt%. Also, an increase of more than 5 wt% in nano clay leads to a decrease in the buckling load.

References

[1] Wang MS, Pinnavaia TJ (1994) Clay-polymer nanocomposites formed from acidic derivatives of montmorillonite and an epoxy resin. Chem Mater 6(4):468-474.

[2] Lan T, Kaviratna PD, Pinnavaia TJ (1994) On the nature of polyimide-clay hybrid composites. Chem Mater 6(4):573–575.

[3] Miyagawa H, Drzal LT (2004) Thermo-physical and Impact Properties of Epoxy Nanocomposites Reinforced by Single-Wall Carbon Nanotubes. Polymer 45(15):5163-5170.

[4] Mahajan D, Desai A, Rafailovich M, Cui MH, Yang NL (2006) Synthesis and Characterization of Nanosized Metal Embedded in Polystyrene Matrix. Compos Part B 37(1):74-80.

[5] Gojny FH, Wichman, MHG, Kopke U, Fiedler B, Schulte K (2004) Carbon Nanotube-Reinforced Epoxy-Composites: Enhanced Stiffness and Fracture Toughness at Low Nanotube Content. Compos Sci Technol 64(15):2363-2371.

[6] Lau KT, Lu M, Li HL, Zhou LM, Hui D (2004) Heat Absorbability of Single-Walled, Coiled and Bamboo Nanotube/Epoxy Nanocomposites. J Mater Sci 39(18):5861-5863.

[7] Park JH, Jana SC (2003) The Relationship between Nano- and Microstructures and Mechanical Properties in PMMA–Epoxy–Nanoclay Composites. Polym 44(7):2091-2100.

[8] Ray SS, Okamoto M (2003) Polymer/Layered Silicate Nanocomposites: A Review from Preparation to Processing. Prog. Polym Sci 28(11):39-1641.

[9] Zhou Y, Pervin F, Biswas MA, Rangari VK, Jeelani S (2006) Fabrication and Characterization of Montmorillonite Clay-filled SC-15 Epoxy. Mater Lett 60(7):869-873.

[10] Lau KT, Lu M, Hui D (2006) Coiled Carbon Nanotubes: Synthesis and Their Potential Application in Advanced Composite Structures. Composites Part B 37(6):437-448.

[11] Koizumi M (1997) FGM Activities in Japan. Compos. Part B Eng 28:1-4.

[12] Wang Y, Wu D (2016) Thermal effect on the dynamic response of axially functionally graded beam subjected to a moving harmonic load. Acta Astronaut 127:171-181.

[13] Gupta A, Talha M (2015) Recent development in modeling and analysis of functionally graded materials and structures. Prog. Aerosp. Sci 79:1–14.

[14] Sahmania S, Safaei B (2019) Nonlinear free vibrations of bi-directional functionally graded micro/nano-beams including nonlocal stress and microstructural strain gradient size effects. Thin Walled Struct 140:342-356.

[15] Arefi M, Bidgoli EMR, Dimitri R, Tornabene F (2018) Free vibrations of functionally graded polymer composite nanoplates reinforced with graphene nanoplatelets. Aerosp. Sci. Technol 81:108-117.

[16] Ke LL, Yang J, Kitipornchai S (2010) Nonlinear free vibration of functionally graded carbon nanotube-reinforced composite beams. Compos Struct 92:676-683.

[17] Tam M, Yang Z, Zhao S, Yang J (2019) Vibration and Buckling Characteristics of Functionally Graded Graphene Nanoplatelets Reinforced Composite Beams with Open Edge Cracks. Materials 12:1412.

[18] Wu Z, Zhang Y, Yao G, Zhou Y (2019) Nonlinear primary and super-harmonic resonances of functionally graded carbon nanotube reinforced composite beams. Int J Mech Sci 321–340.

[19] Bahaadini R, Saidi AR (2018) Aeroelastic analysis of functionally graded rotating blades reinforcedwith graphene nanoplatelets in supersonic flow. Aerosp Sci Technol 80:381-391.

[20] Banic D, Bacciocchi M, Tornabene F, Ferreira AJM (2017) Influence of Winkler-Pasternak Foundation on the Vibrational Behavior of Plates and Shells Reinforced by Agglomerated Carbon Nanotubes. Appl Sci 7:1228.

[21] Holland JH (1975) Adaptation in natural and artificial systems, University of Michigan press, Ann Arbor, Michigan, United State of America.

[22] Wang CM, Reddy JN (2000) Shear Deformable Beams and Plates, Elsevier, Oxford, England.

[23] Reddy JN (2004) Mechanics of Laminated Composite Plates and Shells Theory and Analysis, CRC, New York, United State of America.

[24] Thomas B, Inamdar P, Roy T, Nada BK (2013) Finite Element Modeling and Free Vibration Analysis of Functionally Graded Nanocomposite Beams Reinforced by Randomly Oriented Carbon Nanotubes. Int J Theor Appl Res Mech Eng 2:97-102.

[25] Kozlov G, Dzhangurazov B, Ziakov G, Mikitaev A (2012) The Nanocomposites Polyethylene/organoclay Permeability to Gas Description within the Frameworks of Percolation and Multifractal Models. Chem Technol 6:163-166.

[26] Lei ZX, Liew KM, Yu JL (2013) Free vibration analysis of functionally graded carbon nanotube-reinforced

composite plates using the element-kp-Ritz method in thermal environment. Compos Struc 106:128-138.

[27] Ke LL, Yang J, Kitipornchai S (2013) Dynamic Stability of Functionally Graded Carbon Nanotube-Reinforced Composite Beams. Mech Adv Mater Struc 20: 28-37.

JAST
Journal of Aerospace Science and Technology

Pages:110-118 / Vol. 15/ No. 2 /Summer- Fall 2022

Journal of Aerospace Science and Technology

www:jast.ias.ir

DOI : 10.22034/jast.2022.341613.1118
Submit: 09.05.2022 / Accepted: 08.10.2022
Print ISSN:1735-2134 Online ISSN: 2345-3648